Jagannath University Journal of Science
Volume 11, Number II, December 2024, pp. 58−66
https://jnu.ac.bd/journal/portal/archives/science.jsp
ISSN 3005-4486 (Online), ISSN 2224-1698 (Print)

Double Integration Over a Complex Domain Using Triangular Mesh and Gaussian Quadrature

Research Article

M. Alamgir Hossain

Department of Mathematics, Jagannath University, Dhaka-1100, Bangladesh

DOI: https://doi.org/10.3329/jnujsci.v11i2.84236

Received: 30 October 2024 Accepted: 12 December 2024

ABSTRACT

This paper introduces a novel composite numerical integration method specifically designed for domains with complex nonlinear boundaries, where nonlinear functions define the boundaries. The proposed method aims to evaluate double integrals over such complex domains efficiently. The domain is initially divided into a mesh of uniform or non-uniform triangles, each of which is transformed into a standard triangular finite element using basis functions in a local coordinate system. The standard triangle is further subdivided into right isosceles triangles, facilitating composite numerical integration. Each right isosceles triangle is mapped onto a unit square finite element, where the Gauss-Legendre quadrature rule is employed to evaluate the double integrals. The integrals across the entire domain are computed by summing the contributions from all sub-triangles. Numerical examples are provided to demonstrate the effectiveness and accuracy of the proposed method.

Key words: *Double integrals, Quadrilateral and triangular finite element, Gaussian quadrature, Complex domain, Triangular mesh*

1. Introduction

Numerical integration is essential in numerous scientific, engineering, and mathematical fields, where obtaining exact analytical solutions to integrals is often challenging or even impossible, especially over complex domains. By approximating double integrals, numerical integration facilitates the calculation of volumes and other critical quantities encountered in real-world applications.

The literature review indicates that numerical integration over triangular regions was first introduced by Hammer et al. [1–3] and later extended by Stroud [4]. In finite element methods,

***Corresponding author:** M. Alamgir Hossain
Email: alamgir@math.jnu.ac.bd

triangular elements are commonly employed in numerical integration schemes [5]. Building on Hammer et al.'s work [1–3], Cowper [6] developed Gaussian quadrature formulas for symmetrically positioned integration points. Lethor [7] and Hillion [8] formulated integration for triangles by applying one-dimensional Gauss quadrature rules, and Laursen and Gellert [9] discussed symmetric integration formulas with precision up to the tenth degree.

The literature reveals extensive studies on numerical integration using Gauss quadrature over triangular regions [1–9] and on composite numerical integration over triangular [10–12], quadrilateral regions [13] and polygon [15]. A comprehensive survey by Jayan Sarada and K.V. Nagaraja [14] presents formulas for specific triangular and quadrilateral shapes, which they then generalized for arbitrary polygons. Their approach employs higher-order Gauss-Legendre formulas to achieve greater accuracy. Hossain and Islam [15], introduces a general composite integration rule for arbitrary polygons with high precision. Nevertheless, a comprehensive approach to composite numerical integration over domains with complex nonlinear boundaries has yet to be developed.

In a two-dimensional domain, a nonlinear boundary refers to a boundary whose shape cannot be described by a linear equation of the form $ax + by + c = 0$. Instead, it is defined by equations or curves that involve higher-order terms, trigonometric functions, or other nonlinear relationships between the x and y coordinates. Nonlinear boundaries typically exhibit curved or irregular shapes. For example, the boundary $x^2 + y^2 = r^2$ is nonlinear because it involves squared terms. As noted in the literature [10–15], most existing methods are designed for domains with linear boundaries. Nonlinear boundaries, however, significantly increase the complexity of the problem. To address this challenge, we propose a novel composite numerical integration method specifically designed for domains with complex nonlinear boundaries. Our approach involves constructing a uniform or non-uniform triangular mesh to manage such domains effectively. For this purpose, we utilize DistMesh, a MATLAB tool for generating unstructured triangular meshes, to handle nonlinear domains efficiently [17].

In Section 2, we introduced a novel numerical method for evaluating double integrals over complex domains with nonlinear boundaries. In Section 3, we demonstrated the application of this method with two examples, each evaluated over five different domains. This method is validated through comparison with numerical examples and is implemented using MATLAB. In Section 4, we discussed the numerical results obtained from Section 3. Finally, in Section 5, we presented the conclusions of the study.

2. Formulation of integrals over a complex domain

The integral of an arbitrary function, $f(x, y)$ over an arbitrary domain R is expressed as:

$$I = \int \int_R f(x, y)\ dy\, dx \tag{1}$$

2.1 Decompose Domain R into Triangular Mesh

The arbitrary domain R is decomposed into N number of triangular mesh, refining the mesh where necessary, such as around complex boundaries. Consequently, the integral I in Eq. (1) becomes the sum of N integrals, each defined over a triangular subdomain. For instance, if the region R is a rectangle with a circular hole, a triangular mesh is generated over the domain, with finer mesh near the boundary of the circle, as illustrated in Figure 1. The integral I is the sum of all triangle elements (TE_i where $i = 1, 2, \ldots, N$) then given by:

$$I = \sum_{i=0}^{N} I_i = \sum_{i=0}^{N} \int \int_{TE_i} f(x, y)\ dy\, dx \tag{2}$$

2.2 Map Each Triangle to a Standard Triangular Finite Element

Each triangular element is transformed into a standard triangular finite element using basis functions defined in local coordinates. The integral

I_i from Eq. (2) is then mapped to an integral over the region of the standard triangular element (STE_i) by transforming the vertices of the arbitrary triangular element (x_1, y_1), (x_2, y_2), and (x_3, y_3) to $(-1, -1)$, $(1, -1)$, and $(-1, 1)$, respectively. The standard triangular element STE is defined as:

$$STE_i = \{(\alpha, \beta): -1 \le \beta \le 1, -1 \le \alpha \le -\beta\}.$$

This transformation is performed using the linear triangular finite element basis functions:

$$L_1(\alpha, \beta) = -\frac{1}{2}(\alpha + \beta),\ L_2(\alpha, \beta) = \frac{1}{2}(1 + \alpha),\ \text{and}\ L_3(\alpha, \beta) = \frac{1}{2}(1 + \beta).$$

Therefore, from equation (2), I_i becomes

$$I_i = \int_{-1}^{1}\int_{-1}^{-\beta} f(\alpha, \beta)\left|J_{\alpha\beta}\right| \, d\alpha \, d\beta = \int_{-1}^{1}\int_{-1}^{-\beta} \phi(\alpha, \beta) \, d\alpha \, d\beta, \quad (3)$$

where $\phi(\alpha, \beta) = f(\alpha, \beta)\left|J_{\alpha\beta}\right|$, the coordinate transformation $x = \sum_{j=1}^{3} x_j \, L_j(\alpha, \beta)$ and $y = \sum_{j=1}^{3} y_j \, L_j(\alpha, \beta)$, and the corresponding Jacobian, $J_{\alpha\beta} = \frac{\partial x}{\partial \alpha}\frac{\partial y}{\partial \beta} - \frac{\partial x}{\partial \beta}\frac{\partial y}{\partial \alpha}$.

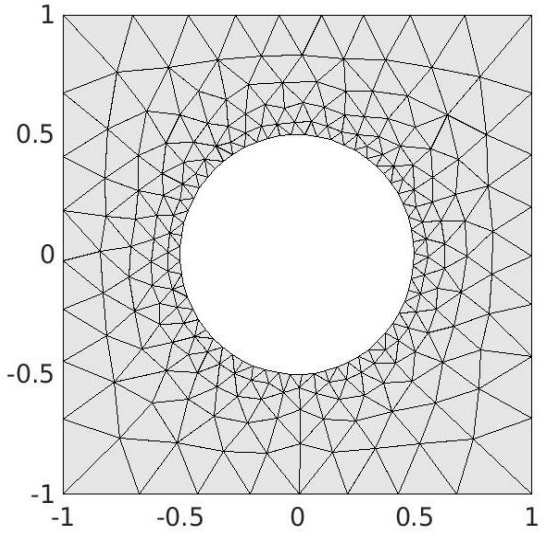

Fig.1 Triangular mesh over a rectangle with circular hole, refined at circle boundary.

2.4 Apply Composite Numerical Integration

We decompose the standard triangular element STE_i in (α, β)-space as described in Eq. (3) into $4 \times m^2$ right isosceles triangles, denoted as IST_k, each with side lengths of $\frac{1}{m}$ [10 – 13]. We apply an affine transformation to convert each right isosceles triangle into a 2-square finite element $[-1, 1] \times [-1, 1]$. Using Gauss-Legendre quadrature, we calculate the sampling points, (λ_a, μ_b), and weight coefficients, (ω_a, ω_b), for numerical integration, where $a, b = 1, 2, \dots, s$ and s is the order of Gauss-Legendre quadrature rule. Finally, we compute the double integral for each triangle using the quadrature points and weight coefficients. Therefore, the integral form (3) is expressed as:

$$I_i = \frac{1}{4m^2}\sum_{a=1}^{s}\sum_{b=1}^{s} \rho_{a,b}\, \psi(x_{a,b}, y_{a,b})$$

where

$$\psi(x_{a,b}, y_{a,b}) = \sum_{i=0}^{2m-1}\sum_{j=0}^{2m-1-i} \phi\left(\frac{x_{a,b} + 2(i-m) + 1}{2m}, \frac{y_{a,b} + 2(j-m) + 1}{2m}\right) + \sum_{i=0}^{2m-2}\sum_{j=0}^{2m-2-i} \phi\left(\frac{-x_{a,b} + 2(i-m) + 1}{2m}, \frac{-y_{a,b} + 2(j-m) + 1}{2m}\right)$$

and $\rho_{a,b} = \frac{1}{4}(2 - \lambda_a - \mu_b)\, \omega_a\, \omega_b$

$$x_{a,b} = \frac{1}{4}\left(-1 + 3\lambda_a - \mu_b(1 + \lambda_a)\right)$$

$$y_{a,b} = \frac{1}{4}\left(-1 + 3\mu_b - \lambda_a(1 + \mu_b)\right)$$

where $a, b = 1, 2, \dots, s$.

3. Numerical Examples

In this section, we evaluate two integrals over the following regions:

(d1) Inside a circle: $R_C = \{(x, y) : x^2 + y^2 \le 1\}$.

(d2) Inside an ellipse: $R_E = \left\{(x, y) : \frac{x^2}{4} + y^2 \le 1\right\}$.

(d3) Inside a square: $R_S = \{(x, y): -1 \le x \le 1, -1 \le y \le 1\}$.

(d4) Inside a polygon, R_p, defined by the vertices (-0.4, -0.5), (0.4, -0.2), (0.4, -0.7), (1.5, -0.4), (0.9, 0.1), (1.6, 0.8), (0.5, 0.5), (0.2, 1), (0.1, 0.4), (-0.7,

0.7) and (-0.4, -0.5).

(d5) A circular hole in a square, i.e., the area outside a circle but inside a square: $R_{CH} = R_S \,/\, R_{Cin} = \{(x,y)\colon (x,y) \in R_S \; and \; (x,y) \notin R_{Cin}\}$

where $R_{Cin} = \{(x,\, y) : x^2 + y^2 < 1\}$ and $R_S = \{(x,y)\colon -1 \le x \le 1,\; -1 \le y \le 1\}$.

Regions (d1) through (d4) are divided into a mesh of uniform triangles, while region (d5) is divided into a mesh of non-uniform triangles (see Figures 2, 3, 4, 5 and 6).

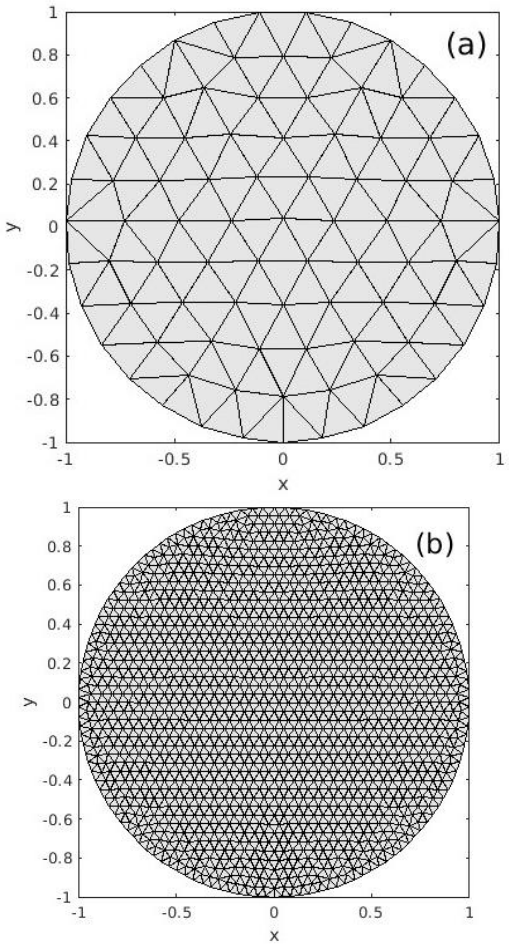

Fig. 2 Uniform triangular mesh over a unit circle R_C: (a) $N = 143$, (b) $N = 2774$.

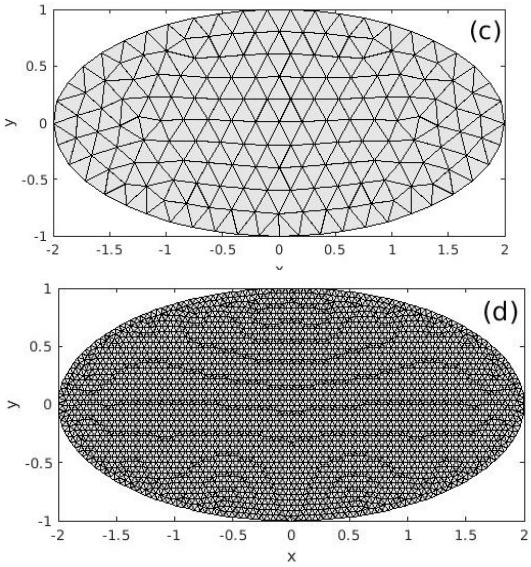

Fig. 3 Uniform triangular mesh over an ellipse R_E: (c) $N = 311$, (d) $N = 5608$.

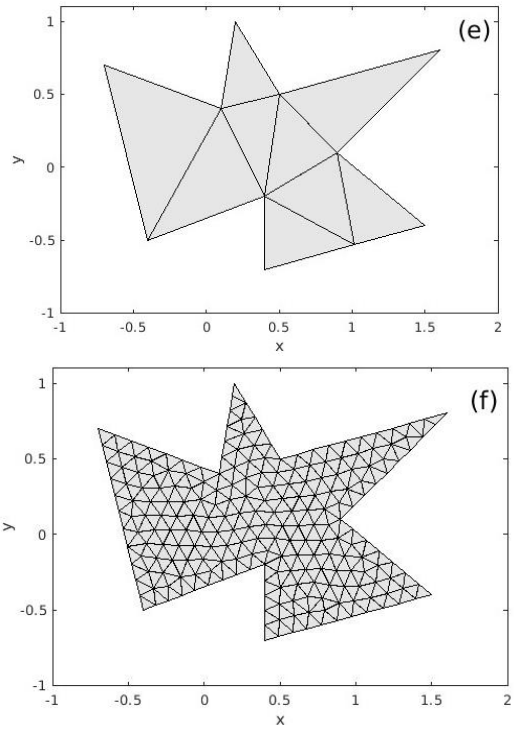

Fig. 4 Uniform triangular mesh on complex polygon R_P: (e) $N = 9$ (f) $N = 378$.

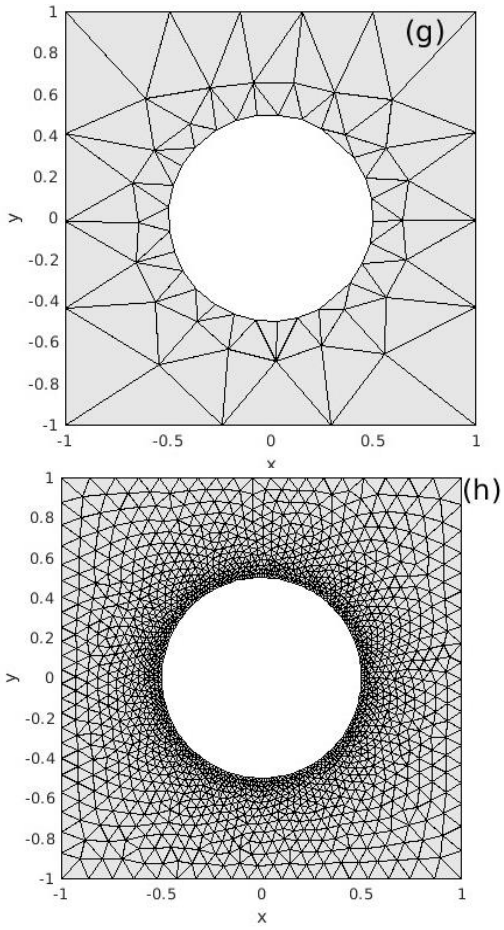

Fig. 5 Non-uniform triangular mesh on rectangular region with a circular hole, refined at the circular boundary R_{CH}: (g) $N = 93$, (h) $N = 2936$.

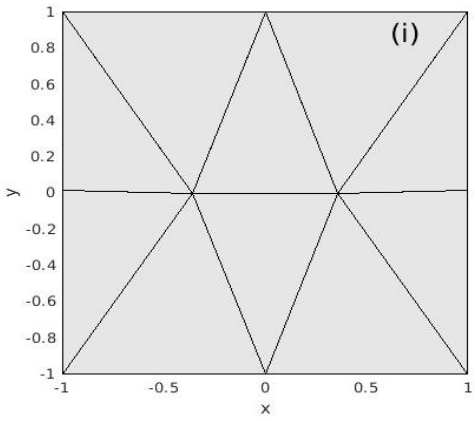

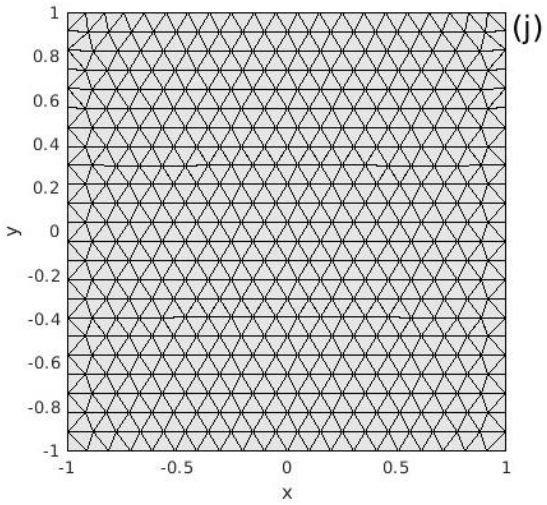

Fig. 6 Uniform triangular mesh over an square R_S: (i) $N = 10$, (j) $N = 899$.

Example 1: Evaluation of $I_1 = \int\int \quad dy\,dx$.

Example 2: Evaluation of

$I_2 = \int\int \frac{c_1x^8+c_2y^9+c_3x^7y^6}{d_1x^9+d_2y^7+d_3}\,dy\,dx$ where $c_1 = \frac{65625}{208}$, $c_2 = \frac{328125}{104}$, $c_3 = \frac{239062}{208}$, $d_1 = 1$, $d_2 = -\frac{125}{4}$ and $d_3 = \frac{175}{4}$.[16]

We denote the double integration for I_1 over the regions R_C, R_E, R_P, and R_{CH} as $I_1^{R_C}$, $I_1^{R_E}$, $I_1^{R_P}$, and $I_1^{R_{CH}}$, respectively. Similarly, the double integrals for I_2 over the regions R_C, R_S, R_P, and R_{CH} in the same way. Table 1 and 2 present the results for integrals I_1 and I_2. For each example, a lower-order Gauss quadrature of order $(s = 3)$ is applied to evaluate the integrals.

Table 1: Evaluation of the integral I_1 over the regions R_C, R_E, R_P, R_{CH} .

Integrals	Initial edge length of triangular elements	Number of triangular elements (TE_i) in the mesh, N	Evaluation of integrals using the proposed method for 4 sub-triangles (IST_k)	Evaluation of integrals using the proposed method for 100 sub-triangles (IST_k)	Exact solution
$I_1^{R_C}$	0.2 [Fig. 2(a)]	143	3.1200435040	3.1359060489	π = 3.1415926 53589793
	0.05 [Fig. 2(b)]	2774	3.1403149656	3.1403149656	
	0.01	71898	3.1415406359	3.1415406359	
	0.005	288935	3.1415796145	3.1415796145	
$I_1^{R_E}$	0.2 [Fig. 3(c)]	311	6.2614670844	6.2614670844	2π = 6.2831853 071795
	0.05 [Fig. 3(d)]	5608	6.2818756914	6.2818756914	
	0.01	144066	6.2831327450	6.2831327450	
	0.005	578397	6.2831720887	6.2831720887	
$I_1^{R_P}$	1 [Fig. 4(e)]	9	1.899999999978	1.8999999999787	1.9
	0.1 [Fig. 4(f)]	378	1.899999999686	1.8999999996865	
$I_1^{R_{CH}}$	0.1 [Fig. 5(g)]	93	3.2229443141123	3.2229443141123	3.2146018 366025
	0.05	481	3.2159672469509	3.2159672469509	
	0.02 [Fig. 5(h)]	2936	3.21482839158	3.21482839158	
	0.01	12058	3.21465864122	3.21465864122	
	0.005	49482	3.21461595617	3.21461595617	
	0.001	1250566	3.214602379	3.214602379	

Table 2: Evaluation of the integral I_2 over the regions R_C, R_S, R_P, R_{CH} .

Integrals	Initial Edge length of triangular elements	Number of triangular elements (TE_i) in the mesh, N	Evaluation of integrals using the proposed method for 4 sub-triangles (IST_k)	Evaluation of integrals using the proposed method for 100 sub-triangles (IST_k)
$I_2^{R_C}$	0.2 [Fig. 2(a)]	143	5.4238889038	5.4241942501
	0.05 [Fig. 2(b)]	2774	5.8253884870	5.8253890940
	0.01	71898	5.8549596569	5.8549596570
	0.005	288935	5.8557489007	5.8557489007

$I_2^{R_S}$ [13, 16]	1	10	19.237011987635	20.817429371742
	0.1	899	20.828491136835	20.828740353281
	0.01	91772	20.82874055109	20.82874055127
$I_2^{R_P}$	1 [Fig. 2(e)]	9	10.9089926539429	10.9130953698007
	0.1 [Fig. 2(f)]	378	10.9130843634477	10.9130950767563
$I_2^{R_{CH}}$	0.1 [Fig. 2(g)]	93	20.7941674121594	20.827541129123
	0.05	481	20.8166341261711	20.827534823139
	0.02 [Fig. 2(h)]	2936	20.8273882341180	20.827518425378
	0.01	12058	20.8275122046300	20.827517609650
	0.005	49482	20.8275162997800	20.827516504240
	0.001	1250566	20.8275171400000	20.827517140000

4. Discussion

The results presented in Tables 1 and 2 showcase the high accuracy and convergence characteristics of the proposed integration method over various complex domains. For each example (d1 through d5), the computed integral values approach the exact solutions as the triangular mesh becomes finer, demonstrating the method's robustness in handling diverse geometric regions, including circles, ellipses, squares, polygons, and regions with holes.

In Example 1, which involves evaluating the integral I_1 over regions R_C, R_E, R_P and R_{CH} show a clear trend of convergence to the known exact values as the number of triangular elements increases. For the integral $I_1^{R_C}$, the results reveal a systematic reduction in error as the initial edge length of triangular elements decreases. For instance, with an initial edge length of 0.2 (143 triangular elements), the evaluation approximates π as 3.1200435040 using 4 sub-triangles, improving to 3.1359060489 with 100 sub-triangles. As the mesh is refined to an edge length of 0.005 (288,935 elements), the result converges to 3.1415796145, closely matching the exact value of $\pi = 3.141592653589793$. Similarly, for $I_1^{R_E}$, representing 2π, the method shows rapid convergence. At an initial edge length of 0.2 (311 elements), the integral evaluates to 6.2614670844. Refining the mesh to 0.005 (578,397 elements) yields 6.2831720887, which is within a small margin of the exact value $2\pi = 6.28318530717952$. The integral $I_1^{R_P}$, with exact value 1.9, also showcases high precision. At an edge length of 1.0 (9 elements), the result is 1.899999999978, maintaining this accuracy even with finer meshes, confirming the method's robustness. For $I_1^{R_{CH}}$, the results validate the method's effectiveness for more complex domains. With an initial edge length of 0.1 (93 elements), the computed value of 3.2229443141123 improves significantly as the mesh is refined to 0.001 (1,250,566 elements), achieving 3.214602379, closely matching the exact value 3.2146018366025.

In Example 2, for the more complex integral expression I_2, the method continues to exhibit convergence and accuracy across each domain. The challenging nature of the rational function evaluated in I_2, especially over domains like R_P and R_{CH}, further demonstrates the method's capacity for handling non-trivial integrands. The second integral, $I_2^{R_C}$, displayed similar trends of $I_1^{R_C}$. With an initial edge length of 0.2, the computed value (5.4238889038) deviated more significantly, but refinement to 0.005 yielded accurate results (5.8557489007). For $I_2^{R_S}$, as the edge length decreased from 1 to 0.01, the computed values converged from 19.237011987635 to 20.82874055109, closely matching the exact solution. Finally, for $I_2^{R_{CH}}$, the proposed method exhibited high precision with increasing mesh refinement. At 0.1, the computed value (20.7941674121594) was close to the exact value, and at 0.001, the computed value (20.827517140000) matched it almost perfectly.

Overall, the proposed method demonstrated robust convergence for both linear and nonlinear boundaries, with finer meshes significantly reducing errors. This highlights the effectiveness of the method in achieving high accuracy in a variety of domains with complex geometries and varying mesh densities.

5. Conclusions

In this paper, we introduced a novel method for evaluating double integrals over arbitrary complex domains with nonlinear boundaries. The method begins by decomposing the domain into a mesh of regular or irregular triangles, enabling flexibility in handling complex geometries. Each triangular element is mapped to a standard triangle using triangular basis functions defined in the local coordinate system and is further subdivided into smaller triangles for enhanced accuracy. These standard triangles are then mapped onto a unit square using quadrilateral basis functions, ensuring uniformity in numerical treatment. For each square, lower-order Gauss quadrature of order ($s = 3$) is applied to evaluate the integrals. This approach ensures precise computation while maintaining computational efficiency. The computed results demonstrate convergence toward exact solutions, even for domains with intricate nonlinear boundaries. Numerical examples highlight the method's robustness and its ability to maintain high accuracy across diverse geometric regions with varying mesh densities.

The proposed method not only balances accuracy and computational efficiency but also offers a systematic framework for handling complex domains, including those with irregular shapes and boundaries. Its convergence properties validate its reliability, making it a suitable and versatile tool for evaluating integrals in engineering, physics, and other applications involving complex domains.

References

1. Hammer P. , Marlowe OJ and Stroud AH. 1956. Numerical integration over simplexes and cones, *Math. Tables and other aids to computation* 10, 130–136.
2. Hammer PC and Stroud AH. 1956. Numerical integration over simplexes, *Math. Tables and other aids to computation* 10, 137–139.
3. Hammer PC and Stroud AH. 1958. Numerical evaluation of multiple integrals, *Math. Tables and other aids to computation* 12, 272–280.
4. Stroud AH. 1974. Numerical Quadrature and Solution of Ordinary Differential Equations, Springer-Verlag, New York Berlin Heidelberg.
5. Zienkiewicz OC. 1977. The Finite Element Method, 3rd Edn.,McGraw Hill Inc.
6. Cowper GR. 1973. Gaussian quadrature formulas for triangles, *Inter. Jn. Numer. Methods Engrs*, 7 , 405–408.
7. Lethor FG. 1976. Computation of double integrals over a triangle, *J. Computational and Applied Mathematics*, 2, 219–224

8. Hillion P. 1977. Numerical integration on a triangle, *Inter. Jn. Numer. Methods Engrs*, 11, 797–815.
9. Lauresn ME and Gellert M. 1978. Some criteria for numerically integrated matrices and quadrature formulas for triangles, *Inter. Jn. Numer. Methods Engrs*, 12, 67–76.
10. Rathod HT, Nagaraja KV and Venkatesudu B. 2007. Symmetric Gauss Legendre quadrature formulas for composite numerical integration over a triangular surface, *Appl. Math. Comput.*,188, 865–876.
11. Rathod HT, Nagaraja KV and Venkatesudu B. 2007. On the application of two symmetric Gauss Legendre quadrature rules for composite numerical integration over a triangular surface, *Appl. Math. Comput.*, 190, 21–39.
12. Islam MS and Hossain MA. 2008. Numerical Integration over an Arbitrary Triangular Region, *International e-Journal of Numerical Analysis and Related Topics (IeJNART)*, Vol 2.
13. Islam MS and Hossain MA. 2009. Numerical Integrations over an Arbitrary Quadrilateral Region, *Appl. Math. Comput.*,Vol. 210, Issue 2, 515-524.
14. Sarada J and Nagaraja KV. 2011. Generalized Gaussian quadrature rules over two-dimensional regions with linear sides, *Appl. Math. Comput.*, 217, 5612–5621.
15. Hossain MA and Islam MS. 2014. Generalized Composite Numerical Integration Rule Over a Polygon Using Gaussian Quadrature, *Dhaka University Journal of Science*,Vol. 62, Issue 1, 25-29.
16. Yagawa G, Ye GW, Yoshimura S. 1990. A numerical integration scheme for finite element method based on symbolic manipulation, Int. J. Numer. Methods Eng. 29 (1990) 1539-1549.
17. Persson PO, Strang G. 2004. A Simple Mesh Generator in MATLAB. *SIAM Review*, Volume 46 (2), pp. 329-345, June 2004